

Filtrates with Hydroxyl Radicals Prepared using Al + Acid + H₂O₂ for Removing Organic Pollutants

Xiao-Han Guo, Yang Yang, and Zhen-Yan Deng*

Cite This: *ACS Omega* 2021, 6, 14182–14190

Read Online

ACCESS |



Metrics & More

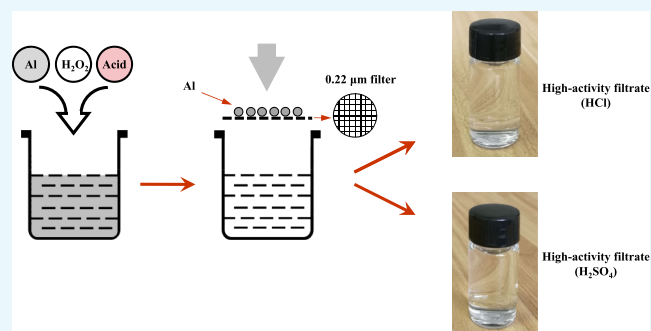


Article Recommendations



Supporting Information

ABSTRACT: In this work, for the first time, high-activity filtrates were prepared by the reaction of aluminum (Al) powder with hydrogen peroxide (H₂O₂) in acidic solution and then filtration, which were used to degrade various organic pollutants such as phenol, methyl orange, and bisphenol A. It was found that the filtrates can effectively degrade and mineralize various organic pollutants and have a high efficiency comparable to their parent Al + acid + H₂O₂ suspensions. The filtrates can keep their high activity for several weeks under ambient conditions, and the activity depends on their initial pH value. At a pH value of ~3.5, the reaction activity of filtrates is the best. Electron spin resonance spectroscopy (ESR) analyses indicated that there is a large quantity of stable hydroxyl radicals (OH•) existing in the filtrates, which are responsible for the removal of organic pollutants. Furthermore, the related factors are discussed.



1. INTRODUCTION

Since Henry J. Fenton found that H₂O₂ could be activated by Fe(II) salts to oxidize tartaric acid in 1894,¹ Fenton and Fenton-like reactions have become of great interest in biological chemistry, synthesis, the chemistry of natural water, and the treatment of hazardous waste.^{2–7} The mechanism behind Fenton reaction was revealed by Haber and Weiss in 1934,⁸ which is to generate hydroxyl radicals (OH•) in aqueous solution. Hydroxyl radicals have a high oxidation potential in the range of 2.8–1.95 V (pH = 0–14) versus standard calomel electrode, which are non-selective and react rapidly with many organic species having rate constants in the range from 10⁸ to 10¹⁰ M⁻¹ s⁻¹.

Advanced oxidation processes (AOPs) were first proposed by Glaze in the 1980s^{9,10} and were defined as processes that generate and use powerful transitory species hydroxyl radicals, where the organic compounds can be oxidized to other species or a total mineralization can take place. In the past few decades, the AOP concept has been extended to the oxidative processes with other radicals such as sulfate (SO₄•⁻), chlorine radicals (Cl•), and so on.^{5,11} In addition to iron, other metals with multiple redox states (such as chromium, cerium, copper, cobalt, manganese, and ruthenium) are also used to decompose H₂O₂ into hydroxyl radicals through a conventional Fenton-like pathway.¹² Meanwhile, the generation of highly reactive oxidizing radicals can be realized by a variety of methods including chemical, photochemical, sonochemical, and electrochemical reactions.^{5,13–15}

Aluminum is a good electron donor^{16–19} and has a more negative redox potential [$E_0(\text{Al}^{3+}/\text{Al}^0) = -1.662 \text{ V}$] than iron

[$E_0(\text{Fe}^{2+}/\text{Fe}^0) = -0.44 \text{ V}$], which has been used to generate hydroxyl and sulfate radicals in aqueous solution and degrade organic pollutants in the past few years.^{20–29} However, there is a dense passive oxide film covering the Al particle surfaces to prevent the transport of electrons from the inner Al to outside target reactants. In order to improve Al reaction activity in aqueous solution, different methods are adopted to activate Al such as acid washing,³⁰ adding polyoxometalate (POM),³¹ with the assistance of Fe(II) ions,^{32,33} mechanical ball milling,^{34–36} and so on.

In this work, Al powder and H₂O₂ were added into an acidic solution to form a suspension and then react for a time period. The suspension was filtrated using a sub-micrometer mesh to obtain a filtrate, which was used to degrade various organic pollutants. For the first time, it was shown that the filtrate has hydroxyl radicals and can effectively degrade and mineralize various organic pollutants and has a high efficiency comparable to its parent suspension.

2. MATERIALS AND METHODS

2.1. Chemicals. Three kinds of high-purity Al powders with the average sizes of 100 nm (Shanghai St-nano Science &

Received: February 12, 2021

Accepted: May 14, 2021

Published: May 26, 2021



Technology Co., China), 4.70 μm (Henan Yuan Yang Aluminum Industry Co., China), and 7.29 μm (High Purity Chemical Co., Tokyo, Japan) were used in this work. Analytical-grade chemicals phenol ($\text{C}_6\text{H}_5\text{OH}$, CAS: 108-95-2), methyl orange (MO, $\text{C}_{14}\text{H}_{14}\text{N}_3\text{NaO}_3\text{S}$, CAS: 547-58-0), bisphenol A (BPA, $\text{C}_{15}\text{H}_{16}\text{O}_2$, CAS: 80-05-7), potassium peroxymonosulfate (PMS, $\text{KHSO}_5 \cdot 0.5\text{KHSO}_4 \cdot 0.5\text{K}_2\text{SO}_4$, CAS: 70693-62-8), aluminum chloride hexahydrate ($\text{AlCl}_3 \cdot 6\text{H}_2\text{O}$, CAS: 7784-13-6), xylenol orange disodium salt ($\text{C}_{31}\text{H}_{30}\text{N}_2\text{Na}_2\text{O}_{13}\text{S}$, CAS: 1611-35-4), hydrogen peroxide (H_2O_2), sulfuric acid (H_2SO_4), hydrochloric acid (HCl), sodium hydroxide (NaOH), tert-butanol (TBA), and anhydrous ethanol (EtOH) were purchased from Sinopharm Chemical Reagent Co., Ltd. (Shanghai, China). All water used in this work was deionized water (resistivity $>18 \text{ M}\Omega \cdot \text{cm}$, $\text{pH} \approx 5.8$).

2.2. Preparation of High-Activity Filtrates. An acidic solution with $\text{pH} = 1$ was prepared by diluting the concentrated HCl or H_2SO_4 solution using deionized water; then, 40 mM H_2O_2 and 4 g L^{-1} 7.29 μm Al powder were added to the diluted acidic solution. The abovementioned suspension was agitated using a magnetic bar with a speed of 500 rpm for 2 h. The reaction temperature is 35 $^\circ\text{C}$, which was controlled using a thermostatic water bath with an accuracy of ± 1 $^\circ\text{C}$. Finally, the high-activity filtrate was obtained by filtrating the suspension using a 0.22 μm polyethersulfone (PES) filter.^{37,38} Figure 1 shows that the high-activity filtrates prepared with HCl and H_2SO_4 are colorless and transparent with a pH value of 3.6 and 3.3, respectively.

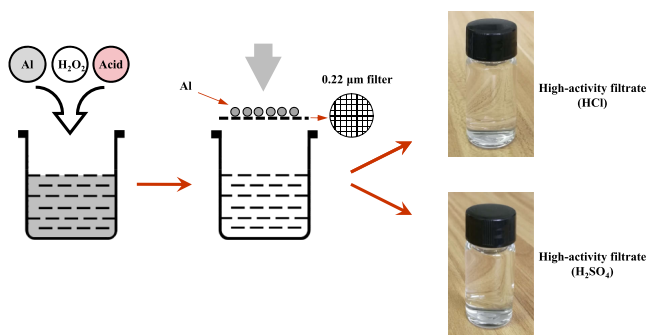


Figure 1. Schematic procedure for preparing the high-activity filtrates.

2.3. Degradation Tests. Three typical organic matters phenol, MO, and BPA were used in the experiment. A suitable amount of organic matter was added into 250 mL of high-activity filtrate filled in a 500 mL Teflon beaker such that the concentration of the organic matter in the solution is 10 mg L^{-1} . The solution was agitated using a magnetic bar with a constant rotating speed of 500 rpm at a temperature of 45 $^\circ\text{C}$. The main absorption peak of organic matter solution at a preset time was measured using an UV–visible absorbance detector (UV–Vis, UV-3600, Shimadzu) through extracting 7 mL of the solution. The organic matter concentration and their main absorption peak height ($\lambda \sim 507$ nm for phenol, $\lambda \sim 464$ nm for MO, and $\lambda \sim 276$ nm for BPA) have a linear correlation, as shown in Figure S1a–c. For the degradation tests of organic matter in Al particle suspension, 7 mL of the extracting sample was filtrated using a 0.22 μm PES filter and then sent for UV–visible absorption measurement. The organic matter degradation ratio α at time t is defined as

$$\alpha = \frac{C_0 - C_t}{C_0} \times 100\% \quad (1)$$

where C_0 is the initial organic matter concentration and C_t is the organic matter concentration at time t . The total organic carbon (TOC) in the filtrate was measured using a total organic carbon analyzer (TOC-L_{CPN}, Shimadzu Co., Japan). The TOC degradation ratio β in the filtrate is written as follows

$$\beta = \frac{C_{\text{TOC},0} - C_{\text{TOC},t}}{C_{\text{TOC},0}} \times 100\% \quad (2)$$

where $C_{\text{TOC},0}$ and $C_{\text{TOC},t}$ are the TOC concentrations at the initial time and time t , respectively.

2.4. Analysis Methods. The morphologies of solid particles were observed via a scanning electron microscope (SU-5000, JEOL); the element analyses of solid particles were performed using an energy-dispersive X-ray spectrometer (INCA Energy 300, Oxford Instruments) equipped on the scanning electron microscope. X-ray diffraction (XRD, D/max-2200, Rigaku) was used to analyze the phase composition of solid powder. The residual Al in the filtrates was measured using an inductively coupled plasma atomic emission spectrometer (ICP-AES, Model no. ICAP 6300, Thermo Fisher Co., USA). The byproducts of the reaction of phenol in the high-activity filtrates were identified using a liquid chromatograph fitted with a mass spectrometer (Qstar XL, AB SCIEX) with a Z-spray electrospray ionization (ESI) source in the negative mode. Electron spin resonance spectrum (ESR) analyses were carried out on a EMX plus spectrometer (Bruker Co., Germany) with 5,5-dimethyl-1-pyrroline-*N*-oxide (DMPO) as a radical spin-trapping reagent.

The particle size distribution in filtrates was measured using a laser particle size analyzer (Zetasizer Lab, Malvern Panalytical, Europe). The Al^{3+} ion concentration in the filtrates was determined using the UV–visible absorbance detector, using xylenol orange disodium (150 mg L^{-1}) as a coloring indicator (Al-XO).³⁹ Standard Al^{3+} ion solution was prepared by dissolving aluminum chloride hexahydrate in deionized water. Our calibration results indicated that the Al^{3+} ion concentration and their main absorption peak height ($\lambda \sim 550$ nm) have a linear correlation, as shown in Figure S1d. Before measurement, the filtrates were diluted with deionized water, so that the Al^{3+} ion concentration in aqueous solution is below the upper limit of the effective measurement.

3. RESULTS AND DISCUSSION

3.1. Al Particle Morphology. Figure S2 shows X-ray diffraction patterns and scanning electron microscopy (SEM) micrographs of as-received 7.29 μm Al powder and those after reaction in HCl + H_2O_2 and H_2SO_4 + H_2O_2 solutions for 2 h, showing that there is no obvious composition change after Al powder was used to prepare the high-activity filtrates. However, a slight corrosion on Al surfaces occurred after Al particles reacted in acid + H_2O_2 solutions, indicating that the consumption of Al is small.

3.2. Oxidizability of Filtrates and Their Parent Suspensions. Figure 2 shows the dependence of the degradation of phenol and the TOC in high-activity filtrates and their parent suspensions on reaction time. It is understood that when Al powder is put into an acidic solution with H_2O_2 ,

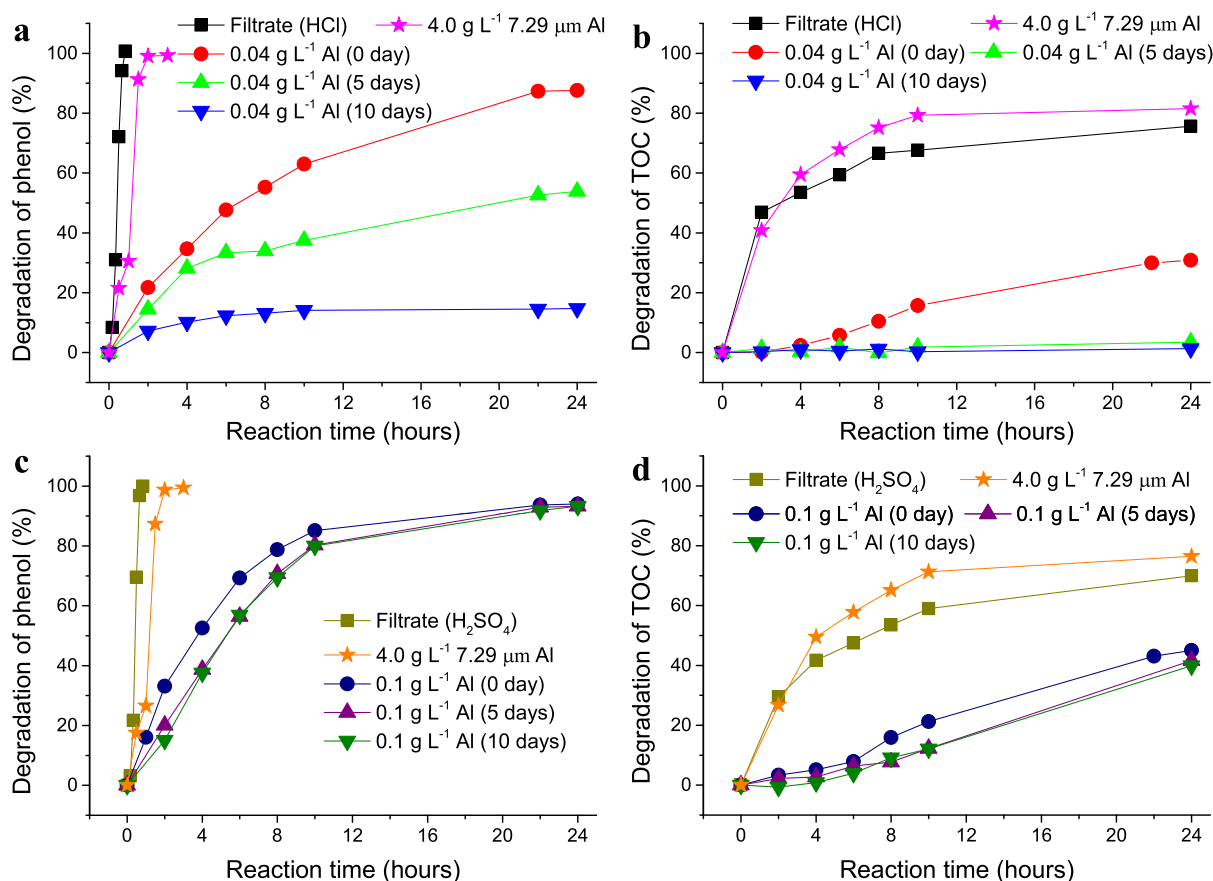
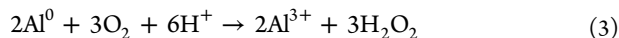


Figure 2. Dependence of the degradation of (a,c) phenol and (b,d) its TOC on reaction time in high-activity filtrates or suspensions with different storage times, where the test temperature is 45 °C, $C_{\text{phenol}} = 10 \text{ mg L}^{-1}$. The “filtrate” was prepared by the reaction of $7.29 \mu\text{m Al} + \text{acid} + \text{H}_2\text{O}_2$ in aqueous solution and then filtration. “ $4.0 \text{ g L}^{-1} 7.29 \mu\text{m Al}$ ” represents the suspension of $7.29 \mu\text{m Al} + \text{acid} + \text{H}_2\text{O}_2$ with $\text{pH} = 1.0$ and $C_{\text{Al}} = 4 \text{ g L}^{-1}$. “ $0.04 \text{ g L}^{-1} \text{ Al}$ ” and “ $0.1 \text{ g L}^{-1} \text{ Al}$ ” represent the suspensions of $100 \text{ nm Al} + \text{acid} + \text{H}_2\text{O}_2$ at $\text{pH} = 3.5$ with $C_{\text{Al}} = 0.04$ and 0.1 g L^{-1} , respectively.

there are hydroxyl radicals generated by the following main processes²⁹



Hydroxyl radicals have a strong oxidation ability to organic matter, and therefore, phenol is degraded, and the TOC decreases with increase in the reaction time in Al + HCl (H_2SO_4) + H_2O_2 suspension. Interestingly, its filtrates also have a strong ability to degrade phenol and the TOC in aqueous solution. It can be seen that it takes $\sim 2 \text{ h}$ to completely remove phenol by the Al + HCl (H_2SO_4) + H_2O_2 suspension, while just 40 min is sufficient to completely decompose phenol with its filtrates. Of course, the TOC removal ratio after 24 h of reaction in the Al + HCl (H_2SO_4) + H_2O_2 suspension is higher than that in its filtrates. These indicate that the Al + HCl (H_2SO_4) + H_2O_2 suspension and its filtrates have a comparable oxidizability to degrade organic pollutants.

In order to test whether the abovementioned phenomena can be extended to other radical system, $2.0 \text{ g L}^{-1} 4.70 \mu\text{m Al}$ powder and 2.0 g L^{-1} PMS were added to deionized water to form a suspension, which was agitated using a magnetic bar with a speed of 500 rpm and reacted at 35 °C for 2 h. By the same procedure in Section 2.2, the reacted Al + PMS suspension was filtrated to obtain a filtrate, which was used

to degrade BPA in aqueous solution. It is known that sulfate radicals ($\text{SO}_4^{\bullet-}$) can be generated in the Al + PMS suspension.^{40,41}

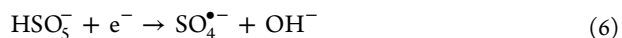
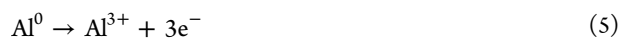


Figure 3 shows that the as-prepared Al + PMS suspension can effectively degrade BPA, while its filtrate almost has no ability to degrade BPA in aqueous solution. This implies that the high oxidation activity does not exist in the filtrate prepared with the Al + PMS suspension.

3.3. Degradation of Different Organic Matters. Figure 4 shows the degradation of different organic matters and their TOC in high-activity filtrates with reaction time. It can be seen that the filtrates just prepared by the reaction of Al powder in acidic solutions without H_2O_2 already degrade phenol up to about 50% within 24 h, although their TOC degradation is negligible. However, the filtrates prepared by the reaction of Al + acid + H_2O_2 suspensions degrade phenol, MO, and BPA very quickly, and their TOC in solution is reduced as high as 40–76% depending on organic matter and the acid used. Meanwhile, the high-activity filtrate prepared with HCl is better than that with H_2SO_4 in degradation and mineralization of organic matter.⁴² The stable products by the reaction of phenol in high-activity filtrates are oxalic and maleic acids shown in Figure S3, which are the same as those of phenol

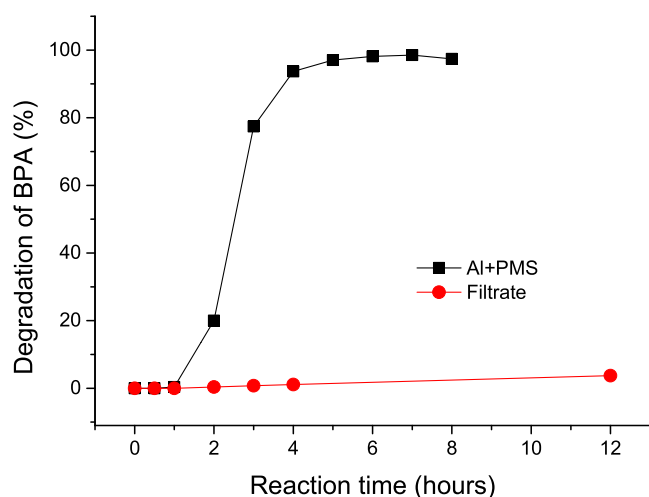


Figure 3. Dependence of the degradation of BPA in the suspension or filtrate on reaction time, where the test temperature is 35 °C, $C_{\text{BPA}} = 20 \text{ mg L}^{-1}$. “Al + PMS” represents the suspension of 4.70 μm Al + PMS with $C_{\text{Al}} = 2.0 \text{ g L}^{-1}$ and $C_{\text{PMS}} = 2.0 \text{ g L}^{-1}$. The “Filtrate” was obtained by filtrating the abovementioned suspension after the reaction of Al and PMS at 35 °C for 2 h.

degradation by Fenton oxidation,^{43,44} where a series of intermediate reactions exist before formation of oxalic and maleic acids,⁴⁴ further confirming the degradation occurrence in the filtrates. TOC removal in high-activity filtrates implies that the organic pollutants are mineralized and decomposed into H_2O and CO_2 .^{43,44}

3.4. Lifetime of High-Activity Filtrates. As-prepared high-activity filtrates were stored under ambient conditions for different times and used for degradation of phenol, as shown in Figure 5. It can be seen that the filtrates keep their high activity for several weeks and can effectively degrade and mineralize phenol in aqueous solutions, although the time for complete degradation of phenol increases and the removal ratio of TOC decreases with the storage time. Meanwhile, the filtrate prepared with H_2SO_4 has a longer lifetime than that prepared with HCl. After a storage time of 20 days and 30 days for high-

activity filtrates prepared with HCl and H_2SO_4 , respectively, the filtrates basically lost their activity.

3.5. Effect of the pH Value. In order to study the effect of the pH value on the stability of high-activity filtrates, a suitable amount of acid (the same as that in preparing the filtrate) or NaOH was added in the as-prepared filtrate. Figure 6 shows the degradation of phenol with reaction time and the removal ratio of its TOC after 24 h in the high-activity filtrate with different pH values. It seems that the filtrates prepared with both HCl and H_2SO_4 are most stable at a pH value of ~ 3.5 . When the pH value becomes more acidic or more alkaline, the reaction activity of filtrates decreases. When the pH value is more than 5.5, the filtrates completely lost their activity. We should mention that the pH value in high-activity filtrates almost has no change after they reacted with organic matter for 24 h.

3.6. ESR Spectrum Analyses. In order to verify the possible existence of hydroxyl radicals in high-activity filtrates, ESR tests with DMPO as a radical spin-trapping reagent were conducted,⁴⁵ as shown in Figure 7. It can be seen that the characteristic peaks of DMPO-OH adducts are noticeable, and these experimental peaks are consistent with those in the theoretical simulation,⁴⁶ as shown in Figure S4, confirming that there are hydroxyl radicals in the high-activity filtrates prepared with both HCl and H_2SO_4 . Figure 7 also shows that the quantity of hydroxyl radicals in high-activity filtrates decreases with increasing their storage time, consistent with the results in Figure 5. At the same time, a radical scavenging experiment with EtOH or TBA was performed to investigate the degradation of phenol in high-activity filtrates, as shown in Figure 8. It is clear that the degradation of phenol was inhibited when EtOH or TBA was added into the solutions, indicating that hydroxyl radicals are the main reactive oxidizing species.

3.7. Related Factors. In order to understand why the filtrates prepared with the Al + acid + H_2O_2 suspension have a high reaction activity, their residual Al and Al^{3+} ion concentrations were analyzed by inductively coupled plasma atomic emission spectrometry (ICP-AES) and Al-XO methods, respectively. The results indicate that the total residual Al in the filtrates prepared with Al + HCl + H_2O_2 and Al + H_2SO_4 +

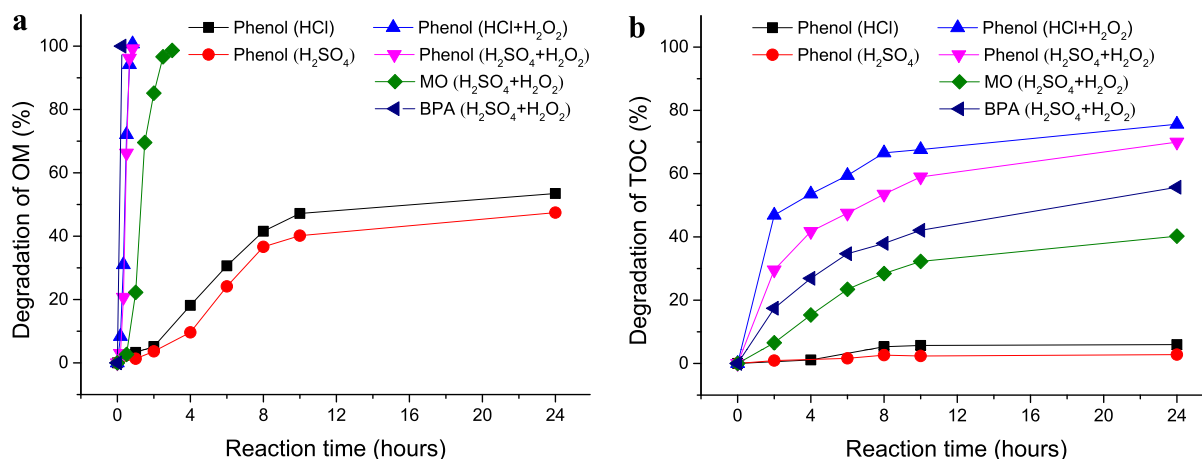


Figure 4. Dependence of the degradation of (a) phenol, MO, and BPA and (b) their TOC in different high-activity filtrates on reaction time, where the test temperature is 45 °C, $C_{\text{phenol}} = C_{\text{MO}} = C_{\text{BPA}} = 10 \text{ mg L}^{-1}$. In parentheses, HCl or H_2SO_4 represents the filtrate prepared by the reaction of Al + acid in aqueous solution and then filtration; HCl + H_2O_2 or H_2SO_4 + H_2O_2 represents the filtrate prepared by the reaction of Al + acid + H_2O_2 in aqueous solution and then filtration.

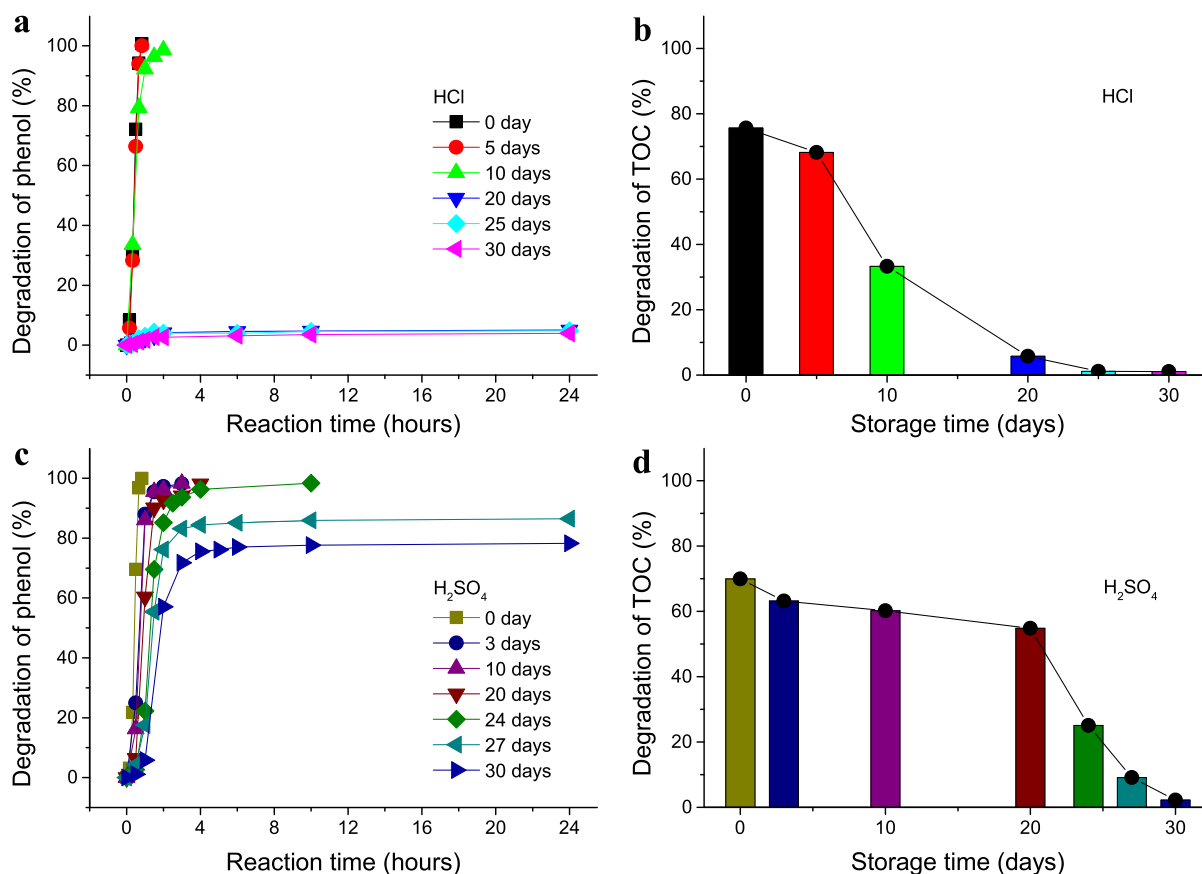


Figure 5. (a,c) Dependence of the degradation of phenol on reaction time in the high-activity filtrate with different storage times. (b,d) Dependence of TOC degradation after phenol reacted in the filtrate for 24 h on its storage time. The test temperature is 45 °C, $C_{\text{phenol}} = 10 \text{ mg L}^{-1}$. HCl (H_2SO_4) represents the filtrate prepared by the reaction of Al + HCl (H_2SO_4) + H_2O_2 in aqueous solution and then filtration.

H_2O_2 suspensions is 38.2 and 75.4 mg L^{-1} , and their corresponding Al^{3+} ion concentration is 39.8 and 79.7 mg L^{-1} , respectively, as listed in Table 1. These show that the residual Al in high-activity filtrates is the dissolved Al^{3+} ions rather than solid metal Al particles. By the way, the solubility of Al^{3+} ions in neutral aqueous solution (<1 ppm) is much lower than that in acidic solution mentioned above.^{37,47} Therefore, the residual Al^{3+} ions in acidic solution can be removed by increasing its pH value after degradation of organic pollutants, for example, by adding lime before the solution is discharged into the environment, such that $\text{Al}(\text{OH})_3$ precipitates are formed.³⁰

As there is a particle size distribution in micrometer-sized Al powder,⁴⁸ in order to further exclude the possibility that the residual Al in high-activity filtrates comes from their Al particles partly passing through the 0.22 μm PES filter, a small amount of nanometer Al powder, comparable with the residual Al in the filtrates, was used to do the experiment. A total of 40 and 100 mg L^{-1} 100 nm Al powder was added into HCl + H_2O_2 (40 mM) and H_2SO_4 + H_2O_2 (40 mM) solutions with pH = 3.5, respectively, which were used to degrade phenol in aqueous solution, as shown in Figure 2. It can be seen that both 40 mg L^{-1} 100 nm Al + HCl + H_2O_2 and 100 mg L^{-1} 100 nm Al + H_2SO_4 + H_2O_2 suspensions can effectively degrade and mineralize 10 mg L^{-1} phenol in aqueous solution. However, their phenol degradation and TOC removal ratios are much lower than those of high-activity filtrates. Furthermore, after the abovementioned two 100 nm Al + acid + H_2O_2 suspensions was stored in air for 10 days, 40 mg

L^{-1} 100 nm Al + HCl + H_2O_2 suspension almost lost its reaction activity, and the activity of 100 mg L^{-1} 100 nm Al + H_2SO_4 + H_2O_2 suspension is much lower than that of the corresponding filtrate stored for the same days, as shown in Figure 5. An intuitive view of high-activity filtrates and the abovementioned two 100 nm Al suspensions after storing for 5 days is shown in Figure S5; it can be seen that the high-activity filtrates are transparent, but the two suspensions are gray, indicating that they are not the similar aqueous solutions. These indicate that hydroxyl radicals in high-activity filtrates are not from the reaction with their residual Al in aqueous solution; they are the stable hydroxyl radicals.

A laser particle size analyzer was used to analyze the as-prepared high-activity filtrates, indicating that there are no particles existing in the filtrate prepared with the Al + H_2SO_4 + H_2O_2 suspension. However, there are a very small amount of unknown particles detected in the filtrate prepared with the Al + HCl + H_2O_2 suspension, with a particle distribution of around 100 nm, as shown in Figure S6, which probably are the AlCl_3 precipitates. Moreover, it is noted that there are some white precipitates deposited at the bottom of the beaker filled with the filtrate prepared with the Al + H_2SO_4 + H_2O_2 suspension after the filtrate was stored for several days. These white precipitates were separated, dried, and then sent for SEM, energy-dispersive X-ray spectrometry (EDS), and X-ray diffraction analyses, as shown in Figure S7. It can be seen that the white precipitates are porous and amorphous $\text{Al}_2(\text{SO}_4)_3$,⁴⁹ which probably came from the oversaturation of Al^{3+} ions in the solution. Because the pH value changes from

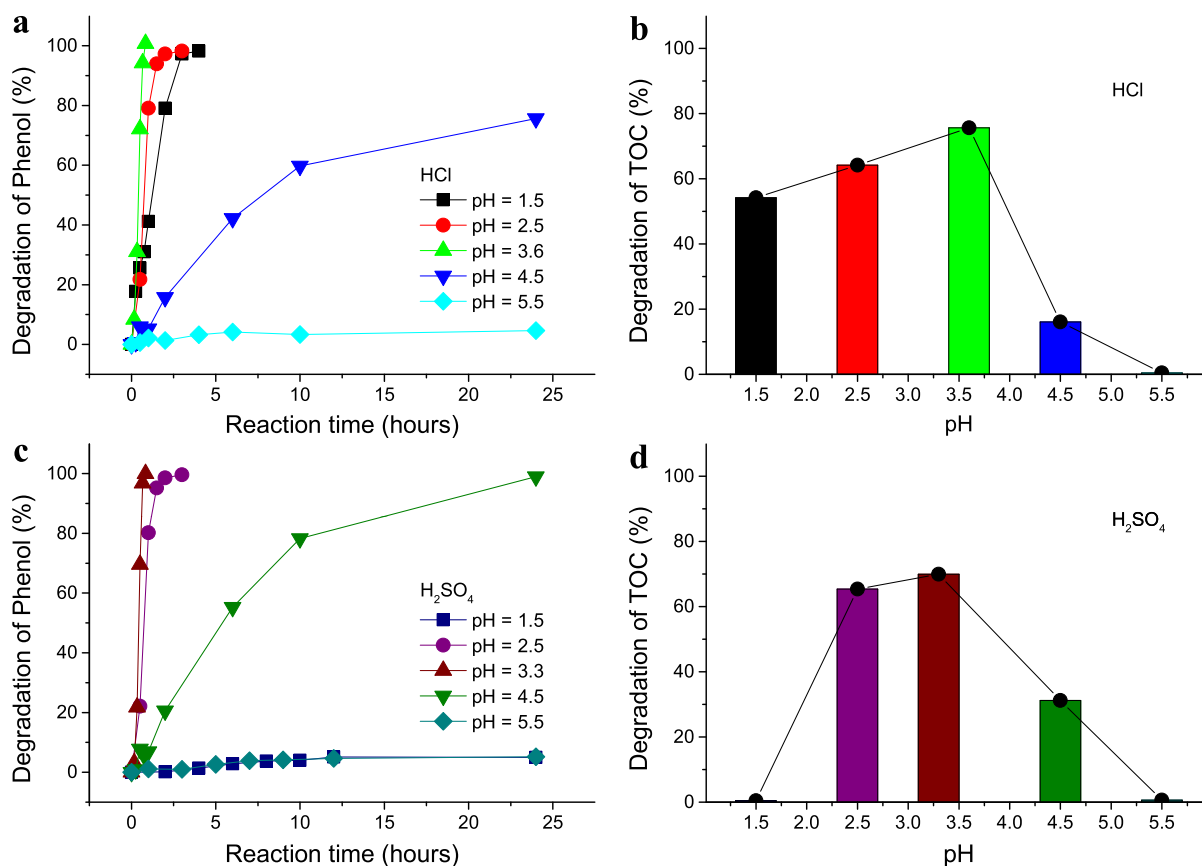


Figure 6. (a,c) Dependence of the degradation of phenol on reaction time in the high-activity filtrate with different pH values. (b,d) Dependence of TOC degradation after phenol reacted in the filtrate for 24 h on the pH value of the filtrate. The test temperature is 45 °C, $C_{\text{Phenol}} = 10 \text{ mg L}^{-1}$. HCl (H_2SO_4) represents the high-activity filtrate prepared by the reaction of $\text{Al} + \text{HCl}$ (H_2SO_4) + H_2O_2 in aqueous solution and then filtration.

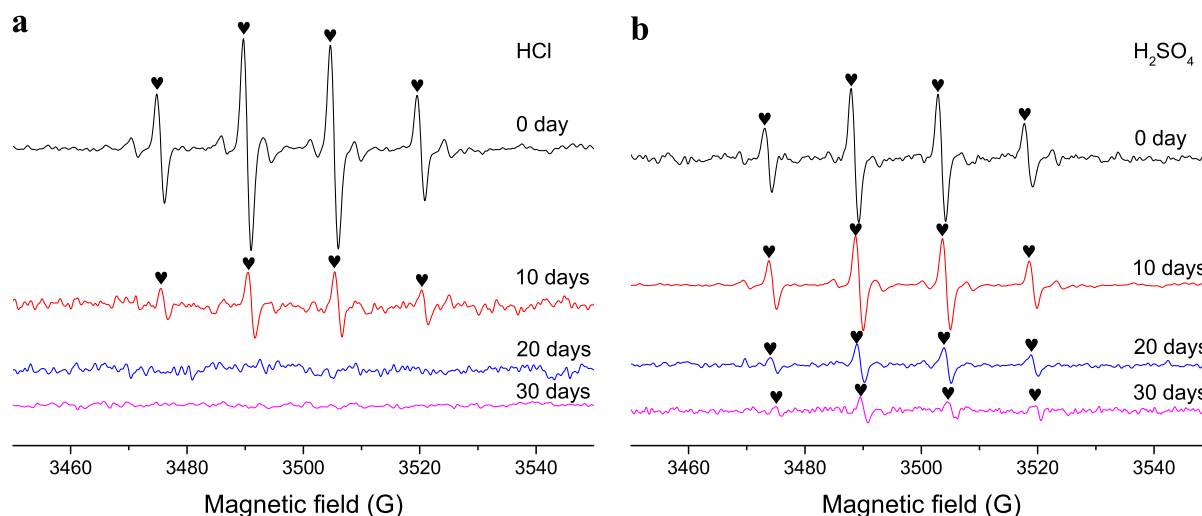


Figure 7. (a,b) ESR spectra of DMPO trapped radical adducts in the high-activity filtrate with different storage times, which was prepared by the reaction of $\text{Al} + \text{HCl}$ (H_2SO_4) + H_2O_2 in aqueous solution and then filtration. The black heart represents DMPO-OH adducts; the concentration of DMPO in the filtrates is 16.7 mM.

1.0 in the initial suspension to 3.3 in its final filtrate, the solubility of Al^{3+} ions decreases rapidly with the increasing pH value in aqueous solution.⁴⁷ The abovementioned analyses further exclude the existence of residual metal Al particles in the high-activity filtrates.

ESR spectra in Figure 7 already confirmed the existence of hydroxyl radicals in the high-activity filtrates, which are

responsible for the degradation of organic pollutants in aqueous solution. Although we have excluded the possibility that the hydroxyl radicals in the filtrates come from the reaction of residual metal Al with H_2O_2 , the mechanisms to form stable hydroxyl radicals in the filtrates are not clear at the moment, which are required to be investigated further. As the existence of hydroxyl radicals in high-activity filtrates is free of

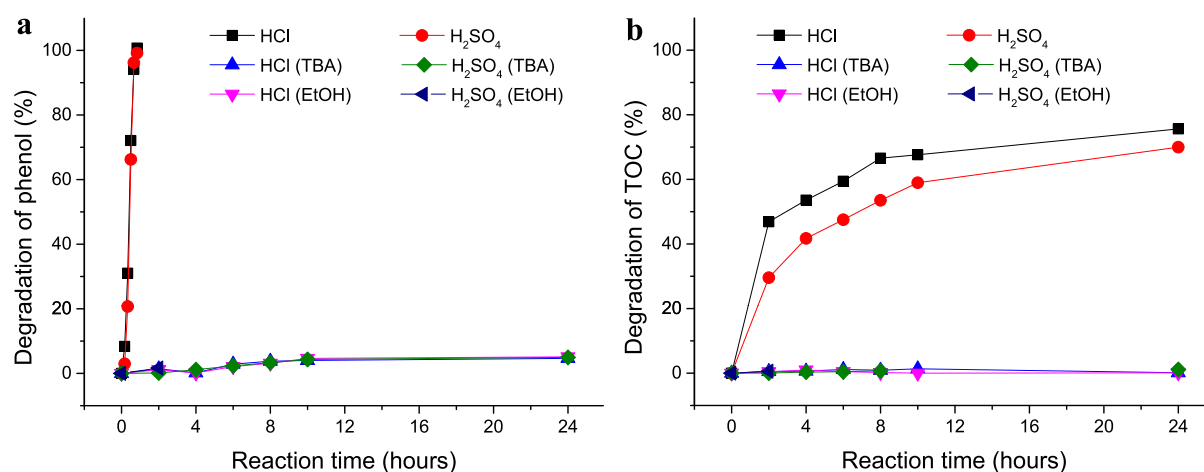


Figure 8. (a,b) Dependence of the degradation of phenol and its TOC on reaction time in the high-activity filtrate with and without a radical scavenger, where HCl (H₂SO₄) represents the high-activity filtrate prepared by the reaction of Al + HCl (H₂SO₄) + H₂O₂ in aqueous solution and then filtration. The test temperature is 45 °C, $C_{\text{Phenol}} = 10 \text{ mg L}^{-1}$, $C_{\text{TBA}} = C_{\text{EtOH}} = 150 \text{ mM}$.

Table 1. Total Amount of Al and Al³⁺ Ion Concentration in the Filtrates

solution	total Al (mg L ⁻¹) measured by ICP-AES	Al ³⁺ ions (mg L ⁻¹) measured by Al-XO
filtrate (HCl)	38.2	39.8
filtrate (H ₂ SO ₄)	75.4	79.7

solid catalysts, the present method make AOP technology more feasible and cost-effective in organic pollutant removal, micro- and nanoelectronic fabrication,^{50,51} biomedical application, and so on.^{3,4}

4. CONCLUSIONS

In this work, for the first time, high-activity filtrates were prepared by a simple method in which Al powder was reacted in acidic solution with H₂O₂ and then filtrated. It was found that the high-activity filtrates have a long lifetime of several weeks and are most stable at a pH value of ~3.5, which can effectively degrade and mineralize different organic pollutants such as phenol, methyl orange, and bisphenol A. ESR spectrum tests have confirmed the existence of hydroxyl radicals (OH[•]) in the filtrates. However, by a similar experimental procedure of Al powder reaction in PMS solution and then filtration, no high-activity filtrate in the sulfate radical system was obtained. The analyses showed that hydroxyl radicals in the filtrates are not from the reaction of residual metal Al with H₂O₂; further investigation is required to clarify the formation mechanisms of stable hydroxyl radicals in aqueous solution.

■ ASSOCIATED CONTENT

Supporting Information

The Supporting Information is available free of charge at <https://pubs.acs.org/doi/10.1021/acsomega.1c00801>.

Linear relationship of UV–Vis–NIR spectroscopy; XRD spectra and SEM images of Al powders; LC/MS spectra of phenol and its intermediates; simulation of ESR spectra; photograph of filtrates and suspensions; particle size distribution in filtrates; SEM image, and XRD and EDS spectra of the precipitates in filtrates (PDF)

■ AUTHOR INFORMATION

Corresponding Author

Zhen-Yan Deng – Energy Materials & Physics Group, Department of Physics, Shanghai University, Shanghai 200444, China; Institute of Low-Dimensional Carbon and Device Physics, Shanghai University, Shanghai 200444, China; orcid.org/0000-0002-4368-7039; Phone: +86-21-66134334; Email: zydeng@shu.edu.cn

Authors

Xiao-Han Guo – Energy Materials & Physics Group, Department of Physics, Shanghai University, Shanghai 200444, China; Institute of Low-Dimensional Carbon and Device Physics, Shanghai University, Shanghai 200444, China

Yang Yang – Energy Materials & Physics Group, Department of Physics, Shanghai University, Shanghai 200444, China; Institute of Low-Dimensional Carbon and Device Physics, Shanghai University, Shanghai 200444, China

Complete contact information is available at: <https://pubs.acs.org/doi/10.1021/acsomega.1c00801>

Notes

The authors declare no competing financial interest.

■ ACKNOWLEDGMENTS

This work is supported by the National Natural Science Foundation of China (grant no. 51872181).

■ REFERENCES

- Fenton, H. J. H. LXXXIII.-Oxidation of tartaric acid in presence of iron. *J. Chem. Soc., Trans.* **1894**, 65, 899–910.
- Pignatello, J. J.; Oliveros, E.; MacKay, A. Advanced oxidation processes for organic contaminant destruction based on the Fenton reaction and related chemistry. *Environ. Sci. Technol.* **2006**, 36, 1–84.
- Yong, L.; Armstrong, K. C.; Dansby-Sparks, R. N.; Carrington, N. A.; Chambers, J. Q.; Xue, Z.-L. Quantitative analysis of trace chromium in blood samples. Combination of the advanced oxidation process with catalytic adsorptive stripping voltammetry. *Anal. Chem.* **2006**, 78, 7582–7587.
- Feng, G.; Cheng, P.; Yan, W.; Boronat, M.; Li, X.; Su, J.-H.; Wang, J.; Li, Y.; Corma, A.; Xu, R.; et al. Accelerated crystallization of zeolites via hydroxyl free radicals. *Science* **2016**, 351, 1188–1191.

- (5) Miklos, D. B.; Remy, C.; Jekel, M.; Linden, K. G.; Drewes, J. E.; Hübner, U. Evaluation of advanced oxidation processes for water and wastewater treatment - A critical review. *Water Res.* **2018**, *139*, 118–131.
- (6) Babu, D. S.; Srivastava, V.; Nidheesh, P. V.; Kumar, M. S. Detoxification of water and wastewater by advanced oxidation processes. *Sci. Total Environ.* **2019**, *696*, 133961.
- (7) Gautam, P.; Kumar, S.; Lokhandwala, S. Advanced oxidation processes for treatment of leachate from hazardous waste landfill: A critical review. *J. Clean. Prod.* **2019**, *237*, 117639.
- (8) Haber, F.; Weiss, J. The catalytic decomposition of hydrogen peroxide by iron salts. *Proc. R. Soc. A* **1934**, *134*, 332–351.
- (9) Glaze, W. H. Drinking-water treatment with ozone. *Environ. Sci. Technol.* **1987**, *21*, 224–230.
- (10) Glaze, W. H.; Kang, J. W. Advanced oxidation processes. Test of a kinetic model for the oxidation of organic compounds with ozone and hydrogen peroxide in a semibatch reactor. *Ind. Eng. Chem. Res.* **1989**, *28*, 1580–1587.
- (11) Deng, Y.; Zhao, R. Advanced oxidation processes (AOPs) in wastewater treatment. *Curr. Pollut. Rep.* **2015**, *1*, 167–176.
- (12) Bokare, A. D.; Choi, W. Review of iron-free Fenton-like systems for activating H₂O₂ in advanced oxidation processes. *J. Hazard. Mater.* **2014**, *275*, 121–135.
- (13) Matilainen, A.; Sillanpää, M. Removal of natural organic matter from drinking water by advanced oxidation processes. *Chemosphere* **2010**, *80*, 351–365.
- (14) Oturan, M. A.; Aaron, J.-J. Advanced oxidation processes in water/wastewater treatment: principles and applications. A review. *Crit. Rev. Environ. Sci. Technol.* **2014**, *44*, 2577–2641.
- (15) Mazivila, S. J.; Ricardo, I. A.; Leitão, J. M. M.; Esteves da Silva, J. C. G. A review on advanced oxidation processes: From classical to new perspectives coupled to two- and multi-way calibration strategies to monitor degradation of contaminants in environmental samples. *Trends Environ. Anal. Chem.* **2019**, *24*, No. e00072.
- (16) Deng, Z.-Y.; Liu, Y.-F.; Tanaka, Y.; Ye, J.; Sakka, Y. Modification of Al particle surfaces by γ -Al₂O₃ and its effect on the corrosion behavior of Al. *J. Am. Ceram. Soc.* **2005**, *88*, 977–979.
- (17) Deng, Z.-Y.; Ferreira, J. M. F.; Tanaka, Y.; Ye, J. Physicochemical mechanism for the continuous reaction of γ -Al₂O₃-modified aluminum powder with water. *J. Am. Ceram. Soc.* **2007**, *90*, 1521–1526.
- (18) Deng, Z.-Y.; Ferreira, J. M. F.; Sakka, Y. Hydrogen-generation materials for portable applications. *J. Am. Ceram. Soc.* **2008**, *91*, 3825–3834.
- (19) Deng, Z.-Y.; Tang, Y.-B.; Zhu, L.-L.; Sakka, Y.; Ye, J. Effect of different modification agents on hydrogen-generation by the reaction of Al with water. *Int. J. Hydrogen Energy* **2010**, *35*, 9561–9568.
- (20) Bokare, A. D.; Choi, W. Zero-valent aluminum for oxidative degradation of aqueous organic pollutants. *Environ. Sci. Technol.* **2009**, *43*, 7130–7135.
- (21) Liu, W.; Zhang, H.; Cao, B.; Lin, K.; Gan, J. Oxidative removal of bisphenol A using zero valent aluminum-acid system. *Water Res.* **2011**, *45*, 1872–1878.
- (22) Zhang, H.; Cao, B.; Liu, W.; Lin, K.; Feng, J. Oxidative removal of acetaminophen using zero valent aluminum-acid system: Efficacy, influencing factors, and reaction mechanism. *J. Environ. Sci.* **2012**, *24*, 314–319.
- (23) Lin, K.; Cai, J.; Sun, J.; Xue, X. Removal of 2,4-dichlorophenol by aluminium/O₂/acid system. *J. Chem. Technol. Biotechnol.* **2013**, *88*, 2181–2187.
- (24) Dogan, M.; Ozturk, T.; Olmez-Hanci, T.; Arslan-Alaton, I. Persulfate and hydrogen peroxide-activated degradation of bisphenol A with nano-scale zero-valent iron and aluminum. *J. Adv. Oxid. Technol.* **2016**, *19*, 266–275.
- (25) Arslan-Alaton, I.; Olmez-Hanci, T.; Khoei, S.; Fakhri, H. Oxidative degradation of Triton X-45 using zero valent aluminum in the presence of hydrogen peroxide, persulfate and peroxymonosulfate. *Catal. Today* **2017**, *280*, 199–207.
- (26) Arslan-Alaton, I.; Olmez-Hanci, T.; Korkmaz, G.; Sahin, C. Removal of iopamidol, an iodinated X-ray contrast medium, by zero-valent aluminum-activated H₂O₂ and S₂O₈²⁻. *Chem. Eng. J.* **2017**, *318*, 64–75.
- (27) Shen, W.; Kang, H.; Ai, Z. Comparison of aerobic atrazine degradation with zero valent aluminum and zero valent iron. *J. Hazard. Mater.* **2018**, *357*, 408–414.
- (28) Khatri, J.; Nidheesh, P. V.; Anantha Singh, T. S.; Suresh Kumar, M. Advanced oxidation processes based on zero-valent aluminium for treating textile wastewater. *Chem. Eng. J.* **2018**, *348*, 67–73.
- (29) Nidheesh, P. V.; Khatri, J.; Anantha Singh, T. S.; Gandhimathi, R.; Ramesh, S. T. Review of zero-valent aluminium based water and wastewater treatment methods. *Chemosphere* **2018**, *200*, 621–631.
- (30) Cheng, Z.; Fu, F.; Pang, Y.; Tang, B.; Lu, J. Removal of phenol by acid-washed zero-valent aluminium in the presence of H₂O₂. *Chem. Eng. J.* **2015**, *260*, 284–290.
- (31) Wu, C. C.; Hus, L. C.; Chiang, P. N.; Liu, J. C.; Kuan, W. H.; Chen, C. C.; Tzou, Y. M.; Wang, M. K.; Hwang, C. E. Oxidative removal of arsenite by Fe(II)- and polyoxometalate (POM)-amended zero-valent aluminum (ZVAL) under oxic conditions. *Water Res.* **2013**, *47*, 2583–2591.
- (32) Hsu, L.-C.; Chen, K.-Y.; Chan, Y.-T.; Deng, Y.; Hwang, C.-E.; Liu, Y.-T.; Wang, S.-L.; Kuan, W.-H.; Tzou, Y.-M. MS title: Catalytic oxidation and removal of arsenite in the presence of Fe ions and zero-valent Al metals. *J. Hazard. Mater.* **2016**, *317*, 237–245.
- (33) Hsu, L.-C.; Cho, Y.-L.; Liu, Y.-T.; Tzou, Y.-M.; Teah, H. Y. Capacity and recycling of polyoxometalate applied in As(III) oxidation by Fe(II)-amended zero-valent aluminum. *Chemosphere* **2018**, *200*, 1–7.
- (34) Ren, T.; Yang, S.; Jiang, Y.; Sun, X.; Zhang, Y. Enhancing surface corrosion of zero-valent aluminum (ZVAL) and electron transfer process for the degradation of trichloroethylene with the presence of persulfate. *Chem. Eng. J.* **2018**, *348*, 350–360.
- (35) Ren, T.; Yang, S.; Wu, S.; Wang, M.; Xue, Y. High-energy ball milling enhancing the reactivity of microscale zero-valent aluminum toward the activation of persulfate and the degradation of trichloroethylene. *Chem. Eng. J.* **2019**, *374*, 100–111.
- (36) Wu, S.; Yang, S.; Liu, S.; Zhang, Y.; Ren, T.; Zhang, Y. Enhanced reactivity of zero-valent aluminum with ball milling for phenol oxidative degradation. *J. Colloid Interface Sci.* **2020**, *560*, 260–272.
- (37) Gai, W.-Z.; Deng, Z.-Y.; Shi, Y. Fluoride removal from water using high-activity aluminum hydroxide prepared by the ultrasonic method. *RSC Adv.* **2015**, *5*, 84223–84231.
- (38) Ge, Y.-L.; Zhang, Y.-F.; Yang, Y.; Xie, S.; Liu, Y.; Maruyama, T.; Deng, Z.-Y.; Zhao, X. Enhanced adsorption and catalytic degradation of organic dyes by nanometer iron oxide anchored to single-wall carbon nanotubes. *Appl. Surf. Sci.* **2019**, *488*, 813–826.
- (39) Zhang, H. Y.; Liu, J.; Zhou, L. H.; Chen, Q.; Liu, J.; Yuan, H. T.; Wang, Y.; Zhao, B.; Zhu, Y. L. A comparison of two methods for determination of Al³⁺. *Hydrometall. China* **2015**, *34*, 347–350.
- (40) Lin, K.-Y. A.; Zhang, Z.-Y. Degradation of bisphenol A using peroxymonosulfate activated by one-step prepared sulfur-doped carbon nitride as a metal-free heterogeneous catalyst. *Chem. Eng. J.* **2017**, *313*, 1320–1327.
- (41) You, J.; Sun, W.; Su, S.; Ao, Z.; Liu, C.; Yao, G.; Lai, B. Degradation of bisphenol A by peroxymonosulfate activated with oxygen vacancy modified nano-NiO-ZnO composite oxides: A typical surface-bound radical system. *Chem. Eng. J.* **2020**, *400*, 125915.
- (42) Alviani, V. N.; Setiani, P.; Uno, M.; Oba, M.; Hirano, N.; Watanabe, N.; Tsuchiya, N.; Saishu, H. Mechanisms and possible applications of the Al-H₂O reaction under extreme pH and low hydrothermal temperatures. *Int. J. Hydrogen Energy* **2019**, *44*, 29903–29921.
- (43) Mani, A.; Kulandaivellu, T.; Govindaswamy, S.; Mohan, A. M. Fe₃O₄ nanoparticle-encapsulated mesoporous carbon composite: An efficient heterogeneous Fenton catalyst for phenol degradation. *Environ. Sci. Pollut. Res.* **2018**, *25*, 20419–20429.

- (44) Villota, N.; Camarero, L. M.; Lomas, J. M.; Perez, J. Changes of turbidity during the phenol oxidation by photo-Fenton treatment. *Environ. Sci. Pollut. Res.* **2014**, *21*, 12208–12216.
- (45) Qi, C.; Yu, G.; Huang, J.; Wang, B.; Wang, Y.; Deng, S. Activation of persulfate by modified drinking water treatment residuals for sulfamethoxazole degradation. *Chem. Eng. J.* **2018**, *353*, 490–498.
- (46) Liu, Y.; Wang, Y.; Cao, P.; Liu, Y. Degradation of edible oil during deep-frying process by electron spin resonance spectroscopy and physicochemical appreciation. *Eur. J. Lipid Sci. Technol.* **2018**, *120*, 1700376.
- (47) Bahena, J. L. R.; Cabrera, A. R.; Valdivieso, A. L.; Urbina, R. H. Fluoride adsorption onto α -Al₂O₃ and its effect on the zeta potential at the alumina-aqueous electrolyte interface. *Sep. Sci. Technol.* **2002**, *37*, 1973–1987.
- (48) Gai, W.-Z.; Liu, W.-H.; Deng, Z.-Y.; Zhou, J.-G. Reaction of Al powder with water for hydrogen generation under ambient condition. *Int. J. Hydrogen Energy* **2012**, *37*, 13132–13140.
- (49) Ghasri-Khouzani, M.; Meratian, M.; Panjepour, M. Effect of mechanical activation on structure and thermal decomposition of aluminum sulfate. *J. Alloys Compd.* **2009**, *472*, 535–539.
- (50) Han, J.; Ji, Q.; Li, H.; Li, G.; Qiu, S.; Li, H.-B.; Zhang, Q.; Jin, H.; Li, Q.; Zhang, J. A photodegradable hexaaza-pentacene molecule for selective dispersion of large-diameter semiconducting carbon nanotubes. *Chem. Commun.* **2016**, *52*, 7683–7686.
- (51) Ji, Q.; Han, J.; Yu, X.; Qiu, S.; Jin, H.; Zhang, D.; Li, Q. Photodegrading hexaazapentacene dispersant for surface-clean semiconducting single-walled carbon nanotubes. *Carbon* **2016**, *105*, 448–453.